International Journal of Thermophysics, Vol. 11, No. 4, 1990

Extension of Thermophysical and Thermodynamic Property Measurements by Laser Pulse Heating up to 10,000 K. II. Under Vacuum[1]

R. W. Ohse[2,3]

The experimental and theoretical efforts for the extension of thermodynamic property measurements up to 10,000 K by a transient-type dynamic laser pulse-heating technique under vacuum (LHV) are reviewed. The technique includes laser pulse heating, mass spectrometry, multiwavelength pyrometry, spectroscopy, high-speed photography, Langmuir probe, and high-tension diode studies. The experimental requirements and applicability limits of this transient technique at extreme rates of evaporation and charged particle emission under hydrodynamic flow conditions are discussed. Special attention is given to the study of the vaporization behavior and equation of state of multicomponent systems, the charged particle emission of ions and electrons, and the gas dynamic expansion mechanism of the evaporating jet. Further applications are the study of the reaction mechanism of combustion processes to investigate their efficiency and pollution.

KEY WORDS: charged particle emission; emissivity; equation of state; evaporation; gas dynamics; high-speed photography; high temperatures; Knudsen technique; Langmuir probe; laser pulse heating; mass spectrometry; pyrometry; thermionic emission; transient heating; work function; vapor pressure.

1. INTRODUCTION

Modern technologies, resource conservations, cost savings, and antipollution requirements in our highly energy-dependent society have led to the

[1] Paper presented at the First Workshop on Subsecond Thermophysics, June 20–21, 1988, Gaithersburg, Maryland, U.S.A.

[2] Commission of the European Communities, Joint Research Centre, Karlsruhe Establishment, European Institute for Transuranium Elements, Postfach 2340, D-7500 Karlsruhe, Federal Republic of Germany.

[3] Present address: Weinbergstrasse 4, D-7770 Überlingen/Bodensee, Federal Republic of Germany.

0195-928X/90/0700-0771$06.00/0 © 1990 Plenum Publishing Corporation

need for new advanced materials to meet the specific technological requirements and for new sources of energy with increased efficiency of thermal conversion to replace traditional fossile fuels [1, 2]. The resulting increase in operating and peak temperatures and more stringent safety demands require an extension of our knowledge on thermophysical and thermodynamic properties to higher temperatures and an increased data reliability [3, 4].

The extension of property measurements up to 5000 and 10,000 K, i.e., far beyond the melting and boiling point of refractory materials and into their critical temperature region, leads to a number of severe constraints imposing short heating times by transient-type dynamic pulse-heating techniques [5] and fast digital data acquisition systems. The type of constraint depends on the property to be measured, the immediate environment of the specimen, and the chosen technique for high-temperature generation. The study of the vaporization behavior of multicomponent systems, i.e., the mass spectrometric determination of the gaseous species and their partial pressures as a function of surface composition and temperature necessitates evaporation into vacuum [6, 8]. Extreme rates of evaporation and charged particle emission under hydrodynamic flow conditions lead to compositional changes at the surface [6, 7, 9, 10], liquid displacement due to the large recoil forces of the evaporating jet, and crack formation caused by the expansion forces within the specimen [11, 12]. The weakly ionized gas of the vapor jet, i.e., the free electrons produced by thermal ionization, may lead to optical absorption of the electromagnetic radiation emitted from the heated surface and limit the applicability of optical pyrometry [6, 13].

A detailed study of the phenomena involved, limitation of the exposure times, and appropriate high-speed diagnostics with adequate temporal and spatial resolution are necessary to guarantee reliability and accuracy of the measurement. High-speed optical pyrometry was found to be the only technique yielding adequate resolution up to temperatures of the order of 5000 K, depending on the degree of ionization. Absorption measurements of the vapor jet at the wavelength of optical pyrometry give direct evidence of the reliability limit of optical pyrometry [13]. Above this limit a deduction of surface temperature from spectroscopic gas measurements, using gas dynamic relationships, seems the most promising method of approach [6].

The laser pulse-heating technique under vacuum (LHV) is presented in Section 2. A detailed study of the various phenomena is given in Section 4. The vaporization behavior and charged particle emission by a mass spectrometric, Langmuir probe, and high-tension diode studies are presented in Section 5.

2. LASER PULSE HEATING UNDER VACUUM: EXPERIMENTAL APPROACH

The application of pulsed laser beam heating either under vacuum as described in this section or under high inert gas pressure as shown in the previous paper (1) depends on the property to be determined. The technique of laser pulse heating under vacuum has first been designed to determine the vaporization behavior and equation of state of multicomponent systems up to 5000 K and above [14–20].

For the investigation of the vaporization behavior the sample is heater under vacuum by a pulsed high-energy laser beam in the nanosecond [21], microsecond [14], and millisecond [22] time scale with multimode or a well-defined Gaussian spatial power density profile [7]. The vapor pressure is obtained from the depth profile [7, 14] and mass spectrometric analysis [8], the recoil pressure [22], Mach disk studies [23, 24], and the time-resolved temperature variation [5]. A theoretical analysis of the fundamental assumptions involved in the three different techniques, in particular of the rate of evaporation related to the equilibrium saturated vapor pressure through the Hertz–Knudsen equation, and the particular gas dynamic models used for each technique has been given by Magill *et al.* (25). The depth measurement proved to be the most accurate technique involving only a small correction factor due to back scattering (approx. 20%).

The properties directly measured or derived are total and partial vapor pressures, spectral and total emittances, heat capacity, enthalpy, and entropy of phase changes. Modifications of this technique allow the measurement of surface tension [26], viscosity, and thermal expansion.

Vapor pressure measurements using the laser pulse-heating technique are based on the Jertz–Knudsen equation

$$\dot{n} = \frac{\alpha_v \alpha_c p_{sat}}{(2\pi m k T)^{1/2}} \tag{1}$$

which relates the measured rate of evaporation into bacuum $\dot{n}$ to the equilibrium saturated vapor pressure p_{sat}, where α_v and α_c are the evaporation and condensation coefficients, k is Boltzmann's constant, and T is the surface temperature [7, 25]. For evaporation from liquid surfaces $\alpha_v \cdot \alpha_c$ is approximately equal to 1. The rate of evaporation into vacuum is determined by the depth measurement of the crater

$$d = \frac{\tau m}{\rho} \dot{n} \tag{2}$$

where τ is the time display of the surface temperature, m the mass of the evaporating molecule, and ρ the density of the condensed phase. The partial pressures are determined by mass spectrometry as shown in Section 5.1.

The schematic display of the experimental technique, given in Fig. 1, summarizes the main items of this instrumentation. A polished sample is heated under high vacuum up to temperatures of 5000 to 10,000 K using a rectangular Nd:YAG laser pulse of 1-μs to 1-ms duration, with a Gaussian spatial power profile obtained by operating in its ground mode (single transversal mode) and power densities of the order of 10^7 W $\cdot$ cm^{-2}. The diameter of the heated target area in the focal spot of the laser beam, defined as $1/e^2$ of the peak height, is of the order of 1 to 3 mm. Electron bombardment allows additional preheating up to 3000 K [11]. The central target temperature is measured by a specially constructed multiwavelength pyrometer described elsewhere [13, 27–29] with a temporal resolution of 10 ns, a spatial resolution of the order of 100 μm, and a temperature resolution of better than 1% at 5000 K. The fast pyrometric temperature signals are stored with nanosecond time resolution on the diode matrix of the transient digitizers. An EAI Quadrupole and Bendix time-of-flight mass spectrometer were used to identify the various neutral and ionized gaseous species in the vapor jet and to determine their partial pressures. The charged particle emission was investigated by a combination of Langmuir probe and high-tension diode studies as described in Section 5.2 [8]. Spectroscopic temperature measurements and high-speed photography of the evaporating jet are required as input data to investigate the gas dynamic expansion mechanism at extreme rates of evaporation and to estimate back-scattering effects due to the transition from the molecular to the hydrodynamic flow [6, 7]. A 1-m focal length grating polychromator was used for spectroscopic measurements of the gas temperature. Four fast photomultipliers connected to the output slit by optical fibers allow a simultaneous recording of four spectral lines emitted by the vapor jet on the transient digitizers. For high-speed photography of the expanding vapor jet a high-speed image converter camera equipped with an image intensifier was used in either the streak mode with speeds of up to 1 ns $\cdot$ mm^{-1} or in the framing mode at up to 10^7 frames/s.

3. ACCURACY REQUIREMENTS

One of the main tasks in nuclear safety analysis is to estimate the maximum energy release in a core disruptive accident of a liquid-metal fast-breeder reactor [5]. The effective amount of thermal energy released during a power transient and converted into mechanical energy depends on

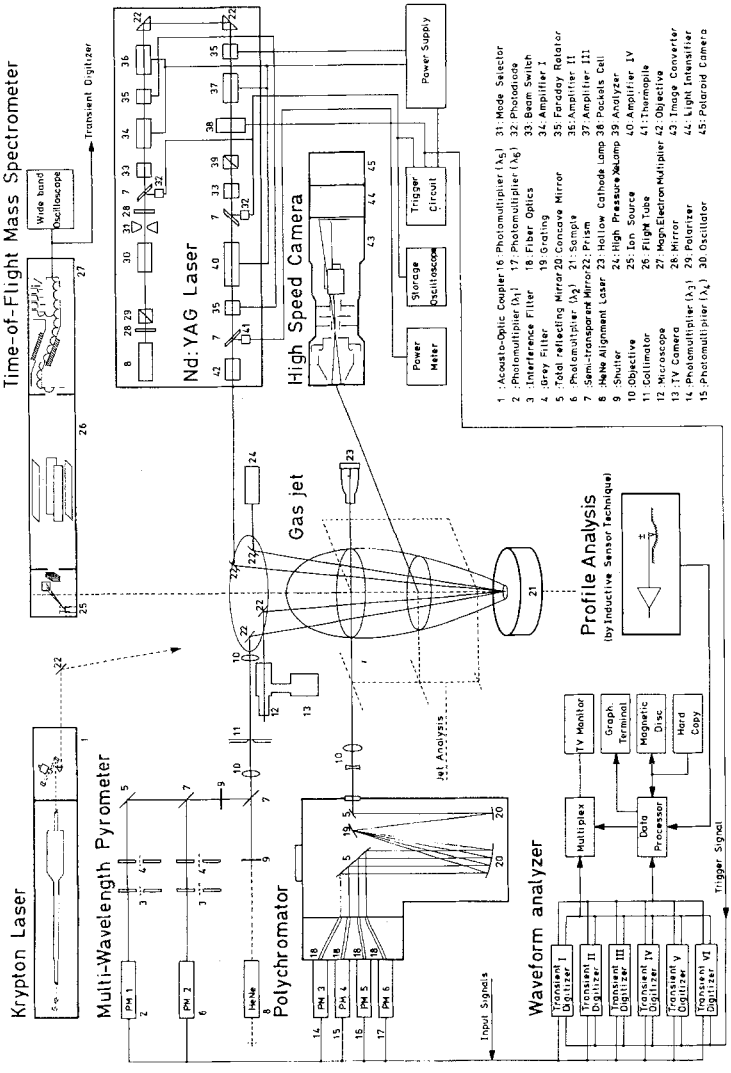

Fig. 1. Schematic setup of laser pulse heating under vacuum (LHV), multiwavelength pyrometry, mass spectromatry, depth profile analysis, spectroscopy, and high-speed photography.

the rate of energy production and the time elapsed between initiating the prompt critical excursion and the disassembly process. Since the disassembly process as a hydrodynamic shutdown mechanism is due mainly to the pressure generation within the fuel pin assembly as the driving force for fuel dispersion and subsequent fuel motion, a "dynamic equation of state" of the irradiated fuel is required. The contribution of fission products to the pressure generated by the pure fuel depends on the burn-up of the fuel, the radial oxygen potential, and the chemical state of the fission products [30, 31]. According to numerous sensitivity studies [5–7, 32–39] of excursion yields on vapor pressure uncertainties, an increase in pressure by a factor of two decreases the energy release by 10–12% depending on the assumptions within the various studies.

4. PROBLEMS ARISING AT EXTREME TEMPERATURES

Classical Knudsen and Langmuir vaporization studies are performed well within the molecular flow region ($\leqslant 1$ Pa) [40–45]. As the temperature is increased far above the melting and boiling point toward the critical point temperature [46, 47], the high rates of evaporation lead to hydrodynamic flow conditions and to depletion effects, i.e., compositional changes at the surface due to noncongruent vaporization which can no longer be restored by diffusion. The large recoil forces of the evaporating jet and temperature gradients across the sample lead to radial liquid displacement and crack formation due to expansion forces within the specimen [12].

4.1. Equilibrium Vapor Pressure under Hydrodynamic Flow Conditions

The problem to be solved is to establish a relationship between the equilibrium vapor pressure and the integrated mass loss under hydrodynamic flow conditions in the gas phase with its associated density, pressure, and temperature gradients. This requires a gas dynamic analysis of the structure of the evaporating jet to determine the net flux transfer from the solid or liquid phase into the gas phase, which can be reduced due to backscattering of particles from the gas phase back onto the surface.

A kinetic theory description of vapor motion for strong evaporation rates led to the recognition of the existance of three basic regions in the evaporating jet [6, 10]. In the first "inner" collision-dominated region, the nonequilibrium regime (Knudsen layer), of approximately 200 mean free paths from the interphase boundary up to the sonic line, the vapor cannot reach supersonic speeds and stays in the subsonic flow motion. The analysis of a one-component system shows that for sonic evaporation into

vacuum, up to 18% of the emitted molecules are scattered back onto the surface. In the second region, the hydrodynamic regime, approximately 10 cm in thickness (for a mean free path of 10^{-6} cm from a disk 10^{-1} cm in diameter), the Mach number of the jet increases monotonically as the density decreases along the axis. The third or "outer" region up to infinity is characterized by a nearly free molecular flow regime.

The equilibrium vapor pressure at high temperatures is directly related to the measured free evaporation rate only for simple one-component systems. In the case of dissociating multicomponent systems with a polyatomic multispecies gas phase, measurements of the free evaporation rates alone without a detailed kinetic study will, in general, not yield the equilibrium vapor pressure [7]. In these systems evaporation into vacuum can be completely different from that under equilibrium conditions. In other words, the assumption of complete thermodynamic equilibrium between the liquid and the gas as valid under closed-box conditions and calculation of partial pressures using the law of mass action are not valid for nonequilibrium evaporation. Here thermodynamic equilibrium can be assumed only in the gas itself. At high rates of evaporation the concept for forced congruent evaporation (FCE) is introduced, whereby the overall composition (e.g., O/M) in the gas phase must equal that in the bulk material [6, 9]. Knowing by gas dynamic analysis the net flux leaving the surface to the flux, i.e., the gas density at the sonic line, the equations for gas reactions together with the FCE condition can then be solved for any gas temperature for the partial pressures of the various gaseous species at the sonic line. The gas temperature entering into the gas dynamic analysis needs to be measured spectroscopically. In a last step it is necessary to provide the relationship between the saturated vapor pressure and the pressure at the sonic line. Detailed descriptions were given elsewhere [6, 7, 10, 25].

4.2. Extension of Applicability Limit: Elimination of Radial Displacement

The basis of the laser surface heating technique for vapor pressure measurements is that the depth of the crater is directly proportional to the rate of evaporation and thus to the saturated vapor pressure, as shown by Eqs. (1) and (2) in Section 2, and that neither liquid nor plastic radial flow is occurring on the target surface [7, 9, 11–13, 19]. In addition, radial displacement leads to a continuous reestablishment of the temperature profile and surface composition as shown by the temperature oscillations of the fast pyrometric temperature signal [11].

Radial liquid or plastic displacement is caused by the large recoil forces of the evaporating jet at high rates of evaporation and the thermal

stresses, acting along the target surface, due to the large temperature gradients. Liquid or plastic flow depends on the thickness of the liquid or plastic layer formed at the surface and the radial recoil and expansion forces [7, 9, 11, 12]. The layer thickness depends on the penetration depth of the heat wave into the material. The penetration depth is determined by the heat flux into the material, the thermal conductivity and temperature gradient, and the recession speed of the evaporating front, i.e., the rate of evaporation [13, 19]. Since the rate of evaporation increases more rapidly than the speed of the heat wave, the layer thickness is expected to decrease with temperature [11, 13]. The radial recoil and expansion forces increase with temperature and its gradient.

The extension of this technique toward lower temperatures is therefore based on limiting the liquid layer thickness to its minimum value at the steady-state temperature and on pushing the temperature gradient, i.e., the zone of disturbance propagation, to the periphery of the laser heated area, thus avoiding feedback to the enter.

4.2.1. Limitation of Liquid Layer Thickness

Calculations on the temperature profile within the solid [11–14, 19] have shown an increase in liquid layer thickness toward lower temperatures. The radial liquid displacement thus increases with increasing

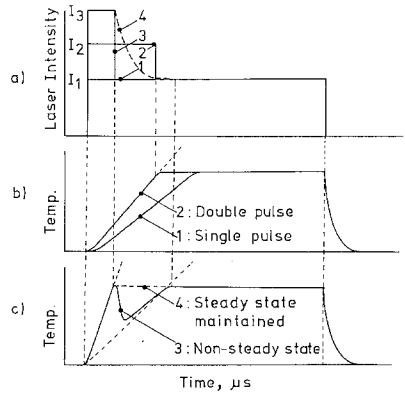

Fig. 2. Reduction of temperature rise time by double-intensity laser pulse-heating technique. (a) Laser intensity versus time; (b) shortest rise time for which a steady-state temperature profile is established; (c) further reduction of temperature rise time by programmed variation of laser intensity with time.

layer thickness but decreases with decreasing rate of evaporation, as the temperature is lowered. The large liquid layers, associated with the low temperatures during the temperature rise time, must therefore be avoided. This was achieved by greatly reducing the temperature rise time by a double-intensity laser pulse-heating technique as schematically shown in Fig. 2 [9, 11, 12]. A high initial power density pulse rapidly raised the temperature to the desired steady-state value, which was then maintained by a second lower-intensity pulse [9, 11, 12, 18]. A further increase in intensity still shortens the temperature rise time, however, after switching to the second intensity, leads to a temperature drop because the heat consumption at the surface by evaporation is fully imposed on the system, although the steady-state profile has not been established. This can be avoided by a programmed lowering to the second "steady-state" intensity [11]. The attainment of steady state with regard to surface temperature, surface compositioon, and rate of evaporation is necessary to achieve accurate rate of evaporation measurements. Under steady-state conditions the heat loss by evaporation, thermal conduction, and radiation is balanced by the laser energy absorbed in the condensed phase.

4.2.2. Shift of Temperature Gradient

The radial recoil and expansion forces increase with temperature and its gradient. Since both thermal conductivity and rate of evaporation and fixed quantities, only the temperature gradient can be changed. In order to ensure that the depth of the crater is directly proportional to the rate of evaporation, i.e., eliminate displacement disturbances from the center of the laser heated target area, the temperature gradient must be shifted to the periphery of the target. This can be achieved only by flattening the spatial power density profile in the laser focal spot [7, 9, 12].

5. VAPORIZATION BEHAVIOR

For a detailed investigation of the high-temperature vaporization behavior and charged particle emission of a multicomponent system with a polyatomic and multispecies vapor phase [42, 48–52], mass spectrometric analysis, Langmuir probe current–voltage characteristics, and high-tension diode studies were applied to identify the various neutral and ionized species, determine their concentrations, and measure the intrinsic electron and ion emission rates [8].

5.1. Mass Spectrometric Analysis

The aim of the mass spectrometric investigations was to identify the gaseous species in the vapor jet, determine their concentrations, and compare the results with thermodynamic equilibrium calculations.

A Bendix time-of-flight and EAI quadrupole mass spectrometer were installed above the laser-heated target for mass analysis of the evaporating jet. The Bendix time-of-flight mass spectrometer, shown in Fig. 1, was used for scanning the spectra at a scan rate of approximately 25 μs, thus allowing an integration of roughly 20 scans per laser pulse. The EAI quadrupole, shown in Fig. 3, allowed to monitor the ion intensity signal at constant mass-to-charge ratio during laser pulse heating. The quantitative removal of ions from the vapor jet by a set of vertical deflection plates (Fig. 3) was controlled by switching off the ionizing current of the ion source. High-energy ions passing both the collection plates and the ion source were collected on a collection plate mounted above the ion source. The electron energy used for ionization was selected according to the appearance and fragmentation potentials of the molecule under investigation. Fragmentation was controlled for each molecule by measuring its ionization efficiency curve [42].

The calibration of the mass spectrometrically measured ion current signals I_i for neutrals according to

$$I_i T = p_{s,i} A \sigma_i k V = p_{s,i} C_i \tag{3}$$

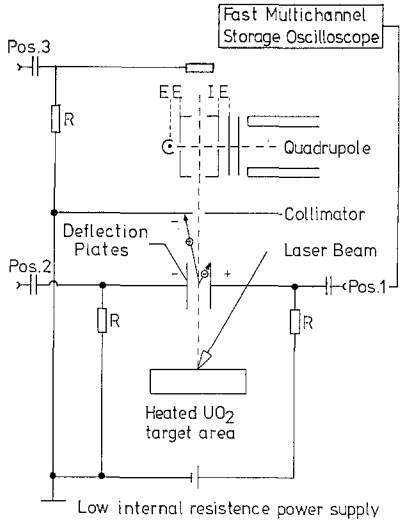

Fig. 3. Mass spectrometric analysis of neutral species and charged particle above the laser heated sample.

wherte A denotes the instrument constant, σ_i the ion cross section, k the conversion factor, and V the multiplier gain, summarized by the ion sensitivity factor C_i, was performed by comparing the ion intensities, measured under steady-state Knudsen effusion conditions to the calculated partial pressure $p_{s,i}$ at temperatures where good agreement among the various vapor pressure measurements has still been achieved (8).

The ion pressures were obtained from the ion currents measured by switching off the ionization current in the ion source. The ion sensitivity factor was determined by Langmuir probe ion density measurements, described in Section 5.2. The ion sensitivity factor, being independent of cross section, was taken equal for all ions. A detailed description of the calibration procedure has been given elsewhere [8].

5.2. Charged Particle Emission

At temperatures of 3500 to 5000 K a large amount of positive ions and electrons was detected by mass spectrometric analysis in the vapor jet above laser pulse-heated uranium dioxide [8]. A combination of Langmuir probe current–voltage characteristics and high-tension diode studies revealed a density of ions larger than the equilibrium values calculated by the Saha equation. The contribution of intrinsic ion emission to the measured rate of evaporation needs to be deduced from the measured rate to calculate the total equilibrium pressure.

5.2.1. Langmuir Probe Current–Voltage Characteristics

The aim of the Langmuir probe measurements was to determine the ion and electron densities and the local electron temperature at various distances from the surface [8]. The Langmuir probe ion density measurements are required to determine the ion sensitivity factor in order to calibrate the mass spectrometric partial ion intensity measurements. Figure 4 gives the experimental setup of the Langmuir probe. The electron temperatures are obtained from the current–voltage characteristics using the relation

$$\frac{d \ln I}{dV} = \frac{e}{kT_e} \tag{4}$$

5.2.2. High-Tension Diode Studies

The aim of the high-tension diode studies was to check whether there is an intrinsic ion emission from the laser-heated surface, to determine the electron and ion work functions, and to clarify whether the charged particle

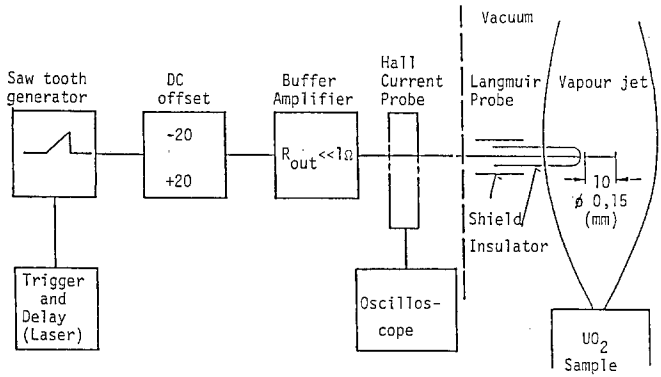

Fig. 4. Experimental setup of Langmuir probe measurement in the laser-produced flowing plasma.

emission depends on the mode of heating by comparing results from resistive and laser pulse heating [8, 53]. The experiments were performed in a temperature range where the vapor pressure is small enough such that the mean free path is larger than the diode spacing (1500 to 2500 K in the case of UO_2). Figure 5 gives the experimental setup for the thermionic emission studies. Electron emission studies on tungsten gave excellent agreement between the electron work function measured by conventional (4.38 eV) and laser heating (4.56 eV) compared to the literature value of 4.52 eV for polycrystalline tungsten [54]. This first measurement of a work function by laser heating showed no evidence of a nonthermal, laser-specific multiphoton absorption effect. In case of UO_2 a concentric filament, first used for preheating the sample to become sufficiently conductive for direct resistive heating, then served as collector in the high-voltage arrangement. The electron work function of UO_2 measured by conventional resistive heating (3.22 eV) agreed well with the literature value of 3.09 eV (55).

6. CONCLUSION

The extension of property measurements of refractory substances to very high temperatures far beyond their melting and boiling points leads to a rapid increase of heat transfer, chemical reactivity, and loss of material strength, imposing short heating times by transient dynamic pulse-heating techniques [2, 5]. Each of these transient techniques was found to introduce its own experimental and interpretational problems asking for a detailed study of the phenomena involved [5]. In each case the

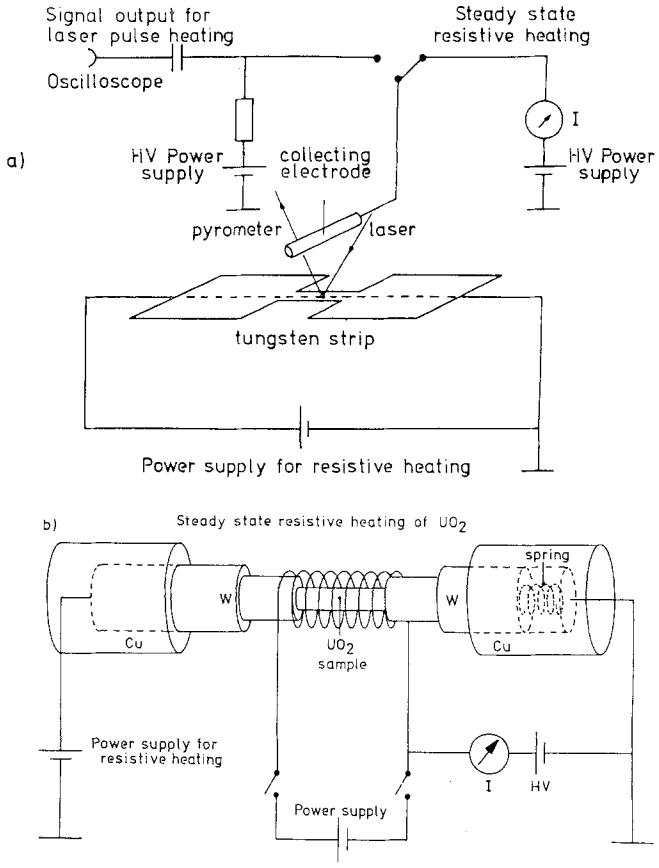

Fig. 5. Experimental setup for thermionic emission studies on (a) tungsten and (b) UO_2 using conventional resistive heating and laser pulse-heating techniques.

appropriate technique has to be chosen on behalf of the property to be measured.

The extension of the vaporization and equation-of-state studies of multicomponent systems up to 5000 and 10,000 K led to a number of severe additional constraints [8] such as extreme rates of evaporation and charged particle emission under hydrodynamic flow conditions with compositional changes at the surface and liquid displacement due to the large recoil forces of the evaporating jet. The transient laser pulse-heating technique involving mass spectrometry, multiwavelength pyrometry, spectroscopy, high-speed photography, Langmuir probe, and high-tension diode studies, proved to be the most accurate technique [25], well suited

to analyze the various problems with adequate spatial and temporal resolution.

The unique advantage of the new laser techniques described in Section 3 of the preceding paper [1, 56] and Section 2 of this paper is their almost-unlimited applicability to high-temperature property measurements due to containment-free high-precision heating up to the critical-point temperatures regardless of the conductive or magnetic properties of the material and their extreme flexibility on experimental diagnostics and on environmental conditions.

Modifications of this technique are well suited to study the effect of heating rate and temperature in combustion processes on the distribution of gaseous products, e.g., the reaction mechanism and decomposition rate in coal pyrolysis, necessary to judge the efficiency and pollution of the process.

The technological importance of high-temperature properties will certainly give strong motivation to both the experimentalist and the theoretician for further refinement of the advanced techniques and model calculations for data prediction in this challenging area of high-temperature materials research. The complexity of the materials' behavior at extreme temperatures and its consequences on transient measurements [1] involves not only basic knowledge on data evaluation [3] and consistency [4] and on dynamic techniques with ultrafast digital data acquisition but practically all specialized topics of high-temperature physics and chemistry. Special attention is required not only on fundamental questions such as phase transformation, solid–liquid–gas interfaces [57], defect structures, or interatomic forces but also on nucleation and growth mechanisms, surface and plasma physics [58], gas dynamics [6, 10], etc. The large variety of disciplines asks for excellent team work and extensive discussions in high-temperature workshops as the one that is part of this Symposium on Thermophysical Properties.

ACKNOWLEDGMENTS

The author would like to express his thanks for contributions to this scientific work to his co-workers J.-F. Babelot, Dr. J.-P. Hiernaut, Dr. J. Magill, and P. Werner, to R. Beukers, F. Capone, W. Heinz, G. Kramer, M. Martellenghi, and R. Selfslag for their assistance in performing the experiments, to the visiting scientists Professor M. Hoch, University of Cincinnati, and Dr. M. Tetenbaum, ANL, USA, and for collaboration to Professor C. Cercignani and Dr. A. Frezzotti, Politecnico di Milano, Dr. M. S. S. Brooks and Dr. C. Ronchi, JRC Karlsruhe, Dr. E. A. Fischer, KfK Karlsruhe, Professor G. DeMaria and Professor L. Mistura, Univer-

sity of Rome, Professor G. J. Hyland, University of Warwick, UK, Dr. P. E. Potter and Dr. M. H. Rand, AERE Harwell, UK, and Professor A. Scotti, JRC Ispra, Italy.

REFERENCES

1. R. W. Ohse, *Int. J. Thermophys.* **11**:753 (1990).
2. R. W. Ohse, *Pure Appl. Chem.* **60**:309 (1988).
3. L. Brewer, in *IUPAC Handbook of Thermodynamic and Transport Properties of Alkali Metals*, R. W. Ohse, ed. (Blackwell Scientific, Oxford, 1985), p. xix.
4. L. Leibowitz and J. K. Fink, in *IUPAC Handbook of Thermodynamic and Transport Properties of Alkali Metals*, R. W. ohse, ed. (Blackwell Scientific, Oxford, 1985), p. xxv.
5. R. W. Ohse, *J. Chem. Soc. Faraday Trans.* **2**(83):1235 (1987).
6. R. W. Ohse, J.-F. Babelot, C. Cercignani, P. R. Kinsman, K. A. Long, J. Magill, and A. Scotti, *NBS Special Publication 561*, J. W. Hastie, ed. (NBS, Washington, D.C., 1979), Vol.1, pp. 83–109; *J. Nucl. Mat.* **80**:232 (1979).
7. R. W. Ohse, J.-F. Babelot, A. Frezzotti, K. A. Long, J. Magill, C. Cercignani, and A. Scotti, *High Temp. Sci.* **13**:35 (1980).
8. R. W. Ohse, J.-F. Babelot, C. Cercignani, J.-P. Hiernaut, M. Hoch, G. J. Hyland, and J. Magill, *J. Nucl. Mat.* **130**:165 (1985).
9. R. W. Ohse, J.-F. Babelot, G. D. Brumme, and P. R. Kinsman, *Rev. Int. Hautés Temp. Réfract.* **15**:319 (1978).
10. C. Cercignani, Report EUR 6843 e (1980).
11. R. W. Ohse, J.-F. Babelot, K. A. Long, and J. Magill, in *Thermodynamics of Nuclear Materials 1979* (IAEA, Vienne, 1980), Vol. I, pp. 171–192.
12. J. Magill, C. Ronchi, J.-F. Babelot, K. A. Long, and R. W. Ohse, *High Temp. High Press.* **12**:503 (1980).
13. R. W. Ohse, J.-F. Babelot, P. R. Kinsman, K. A. Long, and J. Magill, *High Temp. High Press.* **11**:225 (1979).
14. R. W. Ohse, P. G. Berrie, H. G. Bogensberger, and E. A. Fischer, in *Thermodynamics of Nuclear Materials* (IAEA, Vienna, 1975), Vol. I, pp. 307–325.
15. R. W. Ohse, P. G. Berrie, H. G. Bogensberger, and E. A. Fischer, *J. Nucl. Mat.* **59**:112 (1976).
16. H. G. Bogensberger, E. A. Fischer, P. G. Berrie, P. R. Kinsman, and R. W. Ohse, EUR 5501 e (1976); KfK 2272 (1976).
17. R. W. Ohse, P. G. Berrie, G. D. Brumme, and P. R. Kinsman, in *Plutonium 1975 and other Actinides* H. Blank and R. Lindner, eds. (North-Holland, Amsterdam, 1976), pp. 191–200.
18. R. W. Ohse and P. R. Kinsman, *High Temp. High Press.* **8**:209 (1976).
19. R. W. Ohse, J.-F. Babelot, G. D. Brume, and P. R. Kinsman, *Ber. Bunsen-Ges. Phys. Chem.* **80**:780 (1976).
20. J.-F. Babelot, G. D. Brumme, P. R. Kinsman, and R. W. Ohse, *Atomwirtschaft* **22**:387 (1977).
21. N. Asami, M. Nishikawa, and M. Taguchi, in *Thermodynamics of Nuclear Materials* (IAEA, Vienna, 1975), Vol. I, pp. 287–294.
22. M. Bober, H. U. Karow, and K. Schretzmann, in *Thermodynamics of Nuclear Materials* (IAEA, Vienna, 1975), Vol. I, pp. 295–305.
23. H. C. Tsai, A. Covington, and D. R. Olander, *Annual Report LBL* 6016 (1976), p. 188.
24. R. W. Ohse, J.-F. Babelot, A. Frezzotti, K. A. Long, and J. Magill, *High Temp. High Press.* **12**:537 (1980).

25. J. Magill, C. Cercignani, and R. W. Ohse, *High Temp. High Press.* **14**:441 (1982).
26. J. Magill and R. W. Ohse, *J. Nucl. Mat.* **71**:191 (1977).
27. J.-F. Babelot, J. Magill, and R. W. Ohse, in *Temperature, Its Measurement and Control in Science and Industry, Vol. V*, J. F. Schooley, ed. (Am. Inst. Phys., New York, 1982), pp. 439–446.
28. A. Cezairliyan, J.-F. Babelot, J. Magill, and R. W. Ohse, in *Theory and Practice of Radiation Thermometry*, D. P. DeWitt and G. D. Nutter, eds. (John Wiley, New York, 1988), Chap. 8, pp. 529–552.
29. J.-P. Hiernaut, R. Beukers, W. Heinz, R. Selfslag, M. Hoch, and R. W. Ohse, *High Temp. High Press.* **18**:617 (1986).
30. R. W. Ohse and M. Schlechter, in *Behaviour and Chemical State of Irradiated Ceramic Fuels*, Panel Proceedings (IAEA, Vienna, 1974), pp. 299–314; EUR 4893 e (1972).
31. J.-F. Babelot, G. D. Brumme, P. R. Kinsman, and R. W. Ohse, in *Specialists Meeting on the Role of Fission Products in Whole Core Accidents*, IWGFR/19 Summary Report (IAEA, Vienna, 1977), p. 14.
32. D. C. Menzies, TRG Report 1119 (D) (UKAEA, London, 1966).
33. E. J. Robbins, TRG Report 1344 (R) (UKAEA, London, 1966).
34. D. L. Booth, TRG Report 1759 (R/X) (UKAEA, London, 1968/1974).
35. M. J. Gillan, in *Thermodynamics of Nuclear Materials* (IAEA, Vienna, 1975), Vol. I, pp. 269–285.
36. P. Browning, M. J. Gillan, and P. E. Poter, Report AERE-R 8129 (UKAEA, London, 1977).
37. T. F. Bott and J. F. Jackson, *Trans. Am. Nucl. Soc.* **26**:367 (1977).
38. R. W. Ostenson, *Nucl. Technol.* **43**:301 (1979).
39. E. A. Fischer, BNES Conference on Science and Technology of Fast Reactor Safety, Guernsey (May 1986).
40. R. W. Ohse, *J. Chem. Phys.* **44**:1375 (1966); EUR 2166 e (1964); CEA-R-2871 (1965).
41. R. W. Ohse and C. Ciani, in *High Temperature Tecnology* (Butterworth, London, 1967), Proceedings of the Third International Symposium held in Asilomar, California, 1967, pp. 365–375.
42. R. W. Ohse and W. M. Olson, in *Plutonium 1970 and other Actinides*, W. N. Miner, ed. (AIME, New York, 1970), pp. 743–752; EUR 4633 e (1971).
43. J. W. Ward, R. W. Ohse, and R. Reul, *J. Chem. Phys.* **62**:2366 (1975).
44. R. W. Ohse and F. Capone, in *Plutonium 1975 and other Actinides*, H. Blank and R. Lindner, eds. (North-Holland, Amsterdam, 1976), pp. 245–254.
45. M. H. Bradbury and R. W. Ohse, *J. Chem. Phys.* **70**:2310 (1979); *Am. Nucl. Soc. Trans.* **31**:216 (1979).
46. R. W. Ohse and H. v. Tippelskirch, *High Temp. High Press.* **9**:367 (1977).
47. R. W. Ohse, J.-F. Babelot, J. Magill, and M. Tetenbaum, in *IUPAC Handbook of Thermodynamic and Transport Properties of Alkali Metals*, R. W. Ohse, ed. (Blackwell Scientific, Oxford, 1985), Chap. 6.1, pp. 329–347.
48. G. DeMaria, in *Chemical and Mechanical Behavior of Inorganic Materials*, Ragone and Colombo, eds. (Wiley Interscience, New York, 1970), pp. 81–105.
49. R. J. Ackermann, E. G. Rauh, and M. H. Rand, in *Thermodynamics of Nuclear Materials* (IAEA, Vienna, 1980), Vol. I, pp. 11–26.
50. G. Gigli, M. Guido, and G. DeMaria, *J. Nucl. Mat.* **98**:35 (1981).
51. S. K. Gupta and K. Gingerich, *J. Chem. Phys.* **71**:3072 (1979).
52. A. Pattoret, J. Drowart, and S. Smoes, in *Thermodynamics of Nuclear Materials 1967* (IAEA, Vienna, 1968), pp. 613–636.
53. J.-P. Hiernaut, J. Magill, R. W. Ohse, and M. Tetenbaum, *High Temp. High Press.* **17**:633 (1985).

54. M. H. Nichols, *Phys. Rev.* **78**:158 (1950).
55. G. A. Haas and J. T. Jensen, Jr., *J. Appl. Phys.* **34**:3451 (1963).
56. R. W. Ohse, C. Cercignani, A. Frezzotti, J.-P. Hiernaut, M. Hoch, G. J. Hyland, J. Magill, T. Matsui, and P. Werner, *J. Metals* **37**:TMS Annual Meeting 29 (1985).
57. J. Magill, J. Bloem, and R. W. Ohse, *J. Chem. Phys.* **76**:6227 (1982).
58. J. Magill, K. A. Long, M. S. S. Brooks, and R. W. Ohse, in *Proceedings of the 3rd European Conference on Surface Science*, held in Cannes, France, Sept. 1980, Vol. II, Supplément à la Revue "Le Vide, les Couches Minces," No. 201, p. 887.